Binding of Aldolase and Glyceraldehyde-3-Phosphate Dehydrogenase to the Cytoplasmic Tails of *Plasmodium falciparum* Merozoite Duffy Binding-Like and Reticulocyte Homology Ligands

Ipsita Pal-Bhowmick,[a] John Andersen,[a] Prakash Srinivasan,[a] David L. Narum,[b] Jürgen Bosch,[c] and Louis H. Miller[a]

Laboratory of Malaria and Vector Research, National Institute of Allergy and Infectious Diseases, National Institutes of Health, Rockville, Maryland, USA[a]; Laboratory of Malaria Immunology and Vaccinology, National Institute of Allergy and Infectious Diseases, National Institutes of Health, Rockville, Maryland, USA[b]; and Department of Biochemistry and Molecular Biology, Johns Hopkins School of Public Health, and The Johns Hopkins Malaria Research Institute, Baltimore, Maryland, USA[c]

ABSTRACT **Invasion of erythrocytes by *Plasmodium falciparum* requires a connection between the cytoplasmic tail of the parasite's ligands for its erythrocyte receptors and the actin-myosin motor of the parasite. For the thromobospondin-related anonymous protein (TRAP) ligand on *Plasmodium* sporozoites, aldolase forms this connection and requires tryptophan and negatively charged amino acids in the ligand's cytoplasmic tail. Because of the importance of the Duffy binding-like (DBL) and the reticulocyte homology (RH) ligand families in erythrocyte binding and merozoite invasion, we characterized the ability of their cytoplasmic tails to bind aldolase and glyceraldehyde-3-phosphate dehydrogenase (GAPDH), both of which bind actin. We tested the binding of the cytoplasmic peptides of the two ligand families to aldolase and GAPDH. Only the cytoplasmic peptides of some RH ligands showed strong binding to aldolase, and the binding depended on the presence of an aromatic amino acid (phenylalanine or tyrosine), rather than tryptophan, in the context of negatively charged amino acids. The binding was confirmed by surface plasmon resonance analysis and was found to represent affinity similar to that seen with TRAP. An X-ray crystal structure of aldolase at 2.5 Å in the presence of RH2b peptide suggested that the binding site location was near the TRAP-binding site. GAPDH bound to some of the cytoplasmic tails of certain RH and DBL ligands in an aromatic amino acid-dependent manner. Thus, the connection between *Plasmodium* merozoite ligands and erythrocyte receptors and the actin motor can be achieved through the activity of either aldolase or GAPDH by mechanisms that do not require tryptophan but, rather, other aromatic amino acids.**

IMPORTANCE **The invasion of the *Plasmodium* merozoite into erythrocytes is a critical element in malaria pathogenesis. It is important to understand the molecular details of this process, as this machinery can be a target for both vaccine and drug development. In *Plasmodium* sporozoites and *Toxoplasma* tachyzoites, invasion involves a glycolytic enzyme aldolase, linking the cytoplasmic tail domains of the parasite ligands to the actin-myosin motor that drives invasion. This binding requires a tryptophan that cannot be replaced by other aromatic residues. Here we show that aldolase binds the cytoplasmic tails of some *P. falciparum* merozoite erythrocyte-binding ligands but that the binding involves aromatic residues other than tryptophan. The biological relevance of aldolase binding to cytoplasmic tails of parasite ligands in invasion is demonstrated by our observation that RH2b but not RH2a binds to aldolase and, as previously shown, that RH2b but not RH2a is required for *P. falciparum* invasion of erythrocytes.**

Received 16 August 2012 **Accepted** 21 August 2012 **Published** 18 September 2012

Citation Pal-Bhowmick I, et al. 2012. Binding of aldolase and glyceraldehyde-3-phosphate dehydrogenase to the cytoplasmic tails of *Plasmodium falciparum* merozoite Duffy binding-like and reticulocyte homology ligands. mBio 3(5):e00292-12. doi:10.1128/mBio.00292-12.

Editor John Boothroyd, Stanford University

Address correspondence to Louis H. Miller, lmiller@niaid.nih.gov.

Plasmodium falciparum is the causative agent for the most lethal form of human malaria, affecting 500 million people and killing about 1 million children annually. *P. falciparum* belongs to *Apicomplexa*, a monophyletic group of intracellular parasites invading a wide range of host cells but lacking classical means of motility such as a flagellum or cilia (1). The molecular mechanisms underlying *P. falciparum* invasion into erythrocytes are of interest because the invasion machinery can be a target for both vaccine and drug development. However, a complete understanding of the molecular mechanisms underlying the invasion has not yet been achieved. The steps of invasion include attachment in any orientation of the invasive merozoite to the erythrocyte and rapid reorientation to engage ligands in organelles at the parasite's apical end (2, 3). Close apposition cannot occur without binding of these ligands at the apical end to the receptors on the erythrocytes. Following apical reorientation, an interaction between Apical Merozoite Antigen 1 (AMA1) and Rhoptry Neck Protein 2 (RON2) triggers junction formation, as evidenced by the presence of an electron-dense area below the erythrocyte membrane (4). The junction commits the parasite for invasion. The parasite actin-myosin motor functions to bring the merozoite into a vacuole that forms from the erythrocyte membrane as the parasite enters the cell.

In *Toxoplasma gondii* tachyzoites, the surface ligands involved

in invasion were found to be bridged to the actin motor by aldolase (5). Mutations of aldolase that inhibited invasion were shown to affect the binding of the cytoplasmic tail of ligand microneme protein 2 (Mic2) but did not affect glycolytic enzyme activity (6). Subsequently, aldolase was also found to bind to the cytoplasmic tail of thrombospondin-related anonymous protein (TRAP), a ligand on *Plasmodium* sporozoites (7). The critical amino acids in the cytoplasm of TRAP for binding aldolase were a terminal tryptophan and negatively charged amino acids. The structural basis of the binding of the TRAP cytoplasmic tail to aldolase was shown to be a pocket in aldolase for tryptophan and positively charged amino acids in aldolase near the pocket (8). Replacement of the tryptophan with either of the other aromatic amino acids, phenylalanine or tyrosine, greatly reduced or eliminated binding to aldolase (9). The extracellular domains of the ligands TRAP and Mic2 contained von Willebrand A and thrombospondin domains (7). To identify the potential ligands involved in merozoite invasion, a search was conducted in merozoites for von Willebrand A or thrombospondin domains in TRAP or Mic2-like proteins. A protein, Trap-Like Protein-1 (TLP-1), was found that contained both the extracellular domains and the cytoplasmic tail with tryptophan and negatively charged amino acids (10). The cytoplasmic tail bound to aldolase (11), but there was no proteomic evidence that TLP-1 was expressed in the erythrocytic stages (PlasmoDB accession no. PFF0800w) and there was no evidence for its erythrocyte binding (11). A thrombospondin-like domain was found in only two proteins, merozoite Trap-like protein (mTRAP) and PTRAMP, and both had a cytoplasmic tail with tryptophan within negatively charged amino acids (12). However, mTRAP was found not to bind (12) or to bind weakly (13) to erythrocytes and PTRAMP did not bind erythrocytes, indicating that these were probably not invasion ligands.

It is possible that the binding domains in *T. gondii* tachyzoite ligands (e.g., Mic2) and the TRAP ligands on sporozoites evolved together but were lacking in merozoites. Hence, the ligands involved in merozoite invasion of erythrocytes and the mechanism by which these ligands are attached to the parasite actin motor may be distinct from those of TRAP and Mics.

Two families of ligands that appear at the apical end of merozoites are the Duffy binding-like ligands (DBL) that are similar to the *P. vivax* ligand that binds to the Duffy blood group on erythrocytes and the *P. vivax* reticulocyte-like ligands (reticulocyte homologous, or RH [reticulocyte homology]) that bind to reticulocytes (14). In *P. knowlesi* invasion of squirrel monkey erythrocytes, there is also a Duffy-independent invasion pathway (15). The DBL and RH families of ligands in *P. falciparum* can play complementary and cooperative roles in invasion (16, 17). Depending on the parasite clone, most of the receptors can be important, alone or together. The isolates can differ markedly in the receptors that they are able to use when cultured extensively *in vitro* or collected directly from patients in the field (16, 18, 19). Clones are able to switch to different pathways in a genetically stable manner with the expression of different family members (20–22), emphasizing the importance of these DBL and RH family members in *P. falciparum* merozoite invasion.

In *P. falciparum*, there are four DBL genes and five RH genes, only one of which (RH5) lacks a transmembrane region and cytoplasmic domain. These ligands all lack a tryptophan in their cytoplasmic tails that is required for TRAP binding to aldolase. In addition, another glycolytic enzyme, glyceraldehyde-3-phosphate dehydrogenase (GAPDH), has also been shown to bind to actin with affinity similar to that of aldolase (23, 24). *P. falciparum* GAPDH accumulates in the apical region of merozoites, suggesting that it could also play a role in bridging the gap between the DBL and RH ligand cytoplasmic domains and the actin motor (25).

Because of the importance of the DBL and RH family of ligands in erythrocyte binding, we characterized the ability of their cytoplasmic tails to bind to aldolase and to GAPDH. We found that aromatic amino acids other than tryptophan within negatively charged amino acids mediate binding to aldolase and that a different motif that included aromatic amino acids mediated binding to GAPDH. Our studies identify potential merozoite ligands that bridge the gap between the erythrocyte receptor and the parasite actin motor.

RESULTS AND DISCUSSION

The actin-myosin motor system is regarded as a crucial component in apicomplexan invasion (3, 26) and particularly in *Plasmodium* invasion (27, 28). The DBL and RH families of ligands for erythrocyte receptors are important for *P. falciparum* merozoite invasion of erythrocytes. The cytoplasmic tails of members of these two families of ligands on malaria merozoites (14) were tested for binding to aldolase and to GAPDH, two glycolytic enzymes that, in addition to their enzymatic activity, bind actin (24) and thus can potentially bridge the ligands to the actin-myosin motor. Of the eight ligands tested, three (RH1, RH2b, and RH4) bound aldolase (Fig. 1A and 2), and this binding was inhibited in the presence of the aldolase substrate fructose-1,6-bisphosphate (F1-6P).

TRAP was used as a positive control (Fig. 1A and B), showing binding to aldolase in the absence of F1-6P as previously described (7). No binding was observed to TRAP mutants in which the tryptophan was replaced by phenylalanine (W → F) or the negatively charged amino acids were replaced by alanines (E → A) (Fig. 1B), as was shown previously (7, 9). Structural studies demonstrated that tryptophan of TRAP fits snugly into the substrate-binding pocket of aldolase (8). Unlike TRAP, tryptophan was not present in the cytoplasmic tails of the merozoite ligands. Instead, RH1 has a subterminal tyrosine and RH4 has a phenylalanine. When these 2 amino acids were mutated to alanine (RH1 Y → A and RH4 F → A), binding to aldolase was eliminated (Fig. 1C; Table 1). The C terminus of RH2b ends with a tyrosine and phenylalanine; mutation of both to alanine (RH2b YF → AA) completely eliminated binding to aldolase. Mutation of the terminal phenylalanine to alanine (RH2b F → A) had no effect on binding; however, mutation of tyrosine to alanine alone (RH2b Y → A) greatly reduced aldolase binding (Fig. 2). As for TRAP (7), it was noted that negatively charged amino acids were also near the aromatic amino acid. These results establish that members of the RH family can bind aldolase in a tryptophan-independent mechanism. It should be interesting to determine the structure of these peptides bound to aldolase, as they bind through tyrosine or phenylalanine instead of tryptophan.

EBA175 (both 3D7 and cyclic AMP [cAMP] sequences, which differed by 2 amino acids near the end) did not bind aldolase, and mutation of phenylalanine to tryptophan in the cytoplasmic tail of EBA175 did not result in aldolase binding (Fig. 1D; Table 1), showing that not only the amino acids but also the particular combination of the residues and hence the structure of the cyto-

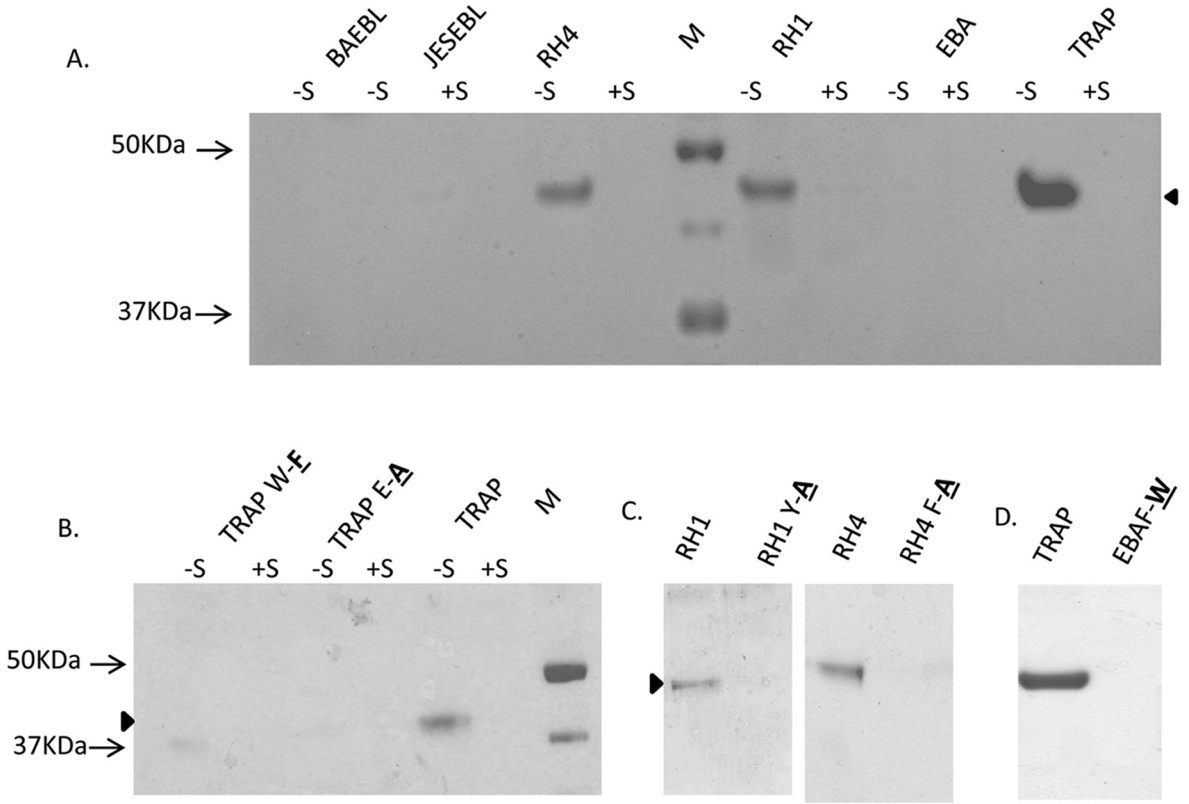

FIG 1 Coomassie-stained gels show the binding of biotinylated peptides of the C terminus of EBA175, BAEBL, JESEBL, RH4, RH1, and TRAP (thromobospondin-related anonymous protein) (Table 1) to rabbit muscle aldolase in the presence or absence of aldolase substrate F1-6P (denoted by +S or –S, respectively). The mutant residues are bold and underlined (see Table 1). Panels A, B, C, and D show separate gels. The molecular mass standards (lane M) 50 kDa and 37 kDa are marked with arrows. An arrowhead marks aldolase.

TABLE 1 The binding of the cytoplasmic tails of malarial ligands and their mutants to rabbit muscle aldolase or yeast GAPDH[a]

Peptide name; mutation(s)	Peptide sequence	RM aldolase binding (no. of expts)	Yeast GAPDH binding (no. of expts)
Reticulocyte homology ligands			
RH1	KQEDKEQEKQQQNDFVCDNN KMDDKSTQKYGRNQEEVMEISFDNDYI	Yes (3)	Yes (3)
RH1; Y-A	KQEDKEQEKQQQNDFVCDNN KMDDKSTQKYGRNQEEVMEISFDND**AI**	No (1)	No (2)
RH2a	NDDVLFKEKDEIIEITFNDNDSTI	No (2)	No (1)
RH2b	NDHLSNYADKEEIIEIVFDENEEKYF	Yes (2)	Minimal (3)
RH2b; Y-A	NDHLSNYADKEEIIEIVFDENEEKAF	Minimal (2)	No (1)
RH2b; F-A	NDHLSNYADKEEIIEIVFDENEEKYA	Yes (2)	No (1)
RH2b; Y,F-A,A	NDHLSNYADKEEIIEIVFDENEEKAA	No (1)	No (1)
RH4	EDEVEDEVEDEDENENEVENENEDFNDI	Yes (4)	Yes (5)
RH4; F-A	EDEVEDEVEDEDENENEVENENEDANDI	No (2)	No (1)/minimal (2)
Duffy binding-like ligands			
EBA175 (3D7)	NQQVQETNINDFSEYHEDINDINFKK	No (3)	No (2)
EBA175 (CAMP)	NQQVQETNINDFSEYHEDINDIKFKI	No (3)	No (2)
EBA175; F-W	NQQVQETNINDFSEYHEDINDIKWKI	No (1)	No (1)
EBA175; K-A	NQQVQETNINDFSEYHEDINDIAFAI	No (1)	ND
BAEBL	NQEVQETNISDYSEYNYNEKNMY	No (2)	Yes (3)
BAEBL; Y-A	NQEVQETNISDYSEYNYNEKNMA	No (2)	No (1)
JESEBL	YMFDQQINVVNSDLYSEGIYDDTTTF	No (3)	Yes (3)
JESEBL; F-A	YMFDQQINVVNSDLYSEGIYDDTTTA	No (2)	No(2)/minimal (1)
TRAP			
TRAP	ETLGEEDKDLDEPEQFRLPEENEWN	Yes (3)	No (2)
TRAP; W-F	ETLGEEDKDLDEPEQFRLPEENEFN	No (1)	No (1)
TRAP; EEE-AAA	ETLGEEDKDLDEPEQFRLPAANAWN	No (1)	ND

[a] Mutant residues are shown in bold. RM, rabbit muscle; GAPDH, glycereladehyde-3-phosphate dehydrogenase; ND, not done. The number of times each experiment was performed is shown in parentheses.

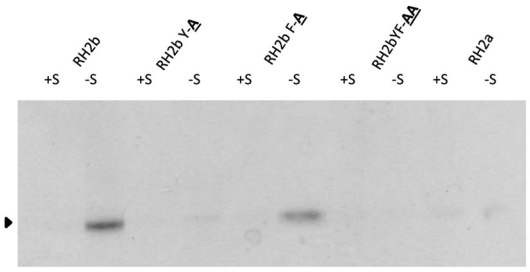

Peptide name	Peptide sequence	Binding
RH2b	NDHLSNYADKEEIIEIVFDENEEKYF	Yes
RH2b Y-**A**	NDHLSNYADKEEIIEIVFDENEEK**A**F	Reduced
RH2b F-**A**	NDHLSNYADKEEIIEIVFDENEEKY**A**	Yes
RH2b Y,F-**AA**	NDHLSNYADKEEIIEIVFDENEEK**AA**	No
RH2a	NDDV-LFKEKDEIIEITFNDNDSTI	No

FIG 2 Coomassie-stained gels show the binding of biotinylated peptides containing the C terminus of RH2a or RH2b peptides and the mutants of RH2b to rabbit muscle aldolase in the presence or absence of aldolase substrate F1-6P (denoted by +S or –S, respectively). The mutant residues are bold and underlined. An arrowhead marks aldolase.

plasmic tail may play a role in the binding. EBA175 contains two positively charged lysines on each side of the phenylalanine, and mutations of the two C-terminal lysines to alanines also did not result in the binding of the mutant EBA175 to aldolase (data not shown). These results are in accord with previous data showing that the cytoplasmic domain of His-tagged EBA175 could not bind aldolase (11). Expression of a chimeric TRAP in which the C-terminal 45 residues of TRAP were replaced by the C-terminal 54 residues of EBA175 yielded *P. berghei* sporozoites that failed to invade mosquito salivary glands. Introduction of a tryptophan in EBA175 did not rescue the invasion. A mutant with an additional, penultimate tryptophan also failed to bind aldolase (11). It was shown earlier that the negative charges of the EBA175 cytoplasmic tail are not important for invasion (29). Those results, along with our results, provide evidence that the cytoplasmic tail of EBA175 cannot substitute for that of TRAP in *Plasmodium* invasion. Moreover, from our data determined with aldolase binders such as RH1, RH2b, and RH4 and nonbinders like EBA175, we can conclude that the presence of an aromatic amino acid, along with the negative charge in the cytoplasmic tail domain, is necessary for aldolase binding. However, tryptophan, along with the negative charge in the cytoplasmic tail domain, is neither necessary nor sufficient for aldolase binding. In addition to bringing the apical end in close apposition with the erythrocytes, EBA175 may play another role, such as signaling, in invasion. It was shown that binding of EBA175 with glycophorin A (glyA) triggers the release of rhoptry proteins and restores cytosolic calcium in merozoites to basal levels (30).

The most direct evidence of the importance of the binding of *Plasmodium* ligands to aldolase was the finding that RH2b but not RH2a is essential for invasion (31), combined with our finding that RH2b but not RH2a binds to aldolase (Fig. 2). RH2a and RH2b have homologous sequences, except for the C-terminal amino acids, including the cytoplasmic tail. Exchange of different regions of the C terminus of RH2a to RH2b demonstrated that the cytoplasmic tail of RH2b was essential for invasion of erythrocytes treated with neuraminidase and trypsin (31). The enzyme treatment of erythrocytes limits alternative pathways of invasion such that RH2b becomes critical for invasion of these enzyme-treated erythrocytes. Although those authors speculated on the importance of the tail in various functions during invasion, they did not consider that it could be important for binding aldolase as a bridge to actin (31), possibly because the cytoplasmic tail of RH2b lacked tryptophan. In our experiments we found that the cytoplasmic tail of RH2a could not bind aldolase, whereas RH2b exhibits such binding (Fig. 2). These data, combined with the data from the exchange of cytoplasmic tails between RH2a and RH2b, highlight the importance of RH2b binding to aldolase for invasion. By extension, the binding of the tails of other ligands may also be important for the attachment to the motor complex.

GAPDH is another glycolytic enzyme that can bind actin (23, 24). The potential for GAPDH as another link to the actin motor was tested by the binding of yeast GAPDH to the cytoplasmic tail of the merozoite ligands. Of the eight ligands tested, four (JESEBL, BAEBL, RH1, and RH4) bound GAPDH. The binding was dependent on either of the aromatic amino acids tyrosine and phenylalanine, depending on the peptide tested (Fig. 3; Table 1). The binding was also blocked by adding the cofactor for GAPDH, NAD reduced form (NADH), showing the specificity of the binding. Immunoprecipitation from a schizont lysate followed by Western probing with antibodies specific to GAPDH showed that antibodies specific to RH1, but not those specific to EBA175, can immunoprecipitate GAPDH (Fig. 3B), confirming our previous pulldown results and also those demonstrating the interaction with *P. falciparum* GAPDH. Other factors in GAPDH binding are unknown, and identification of those factors awaits elucidation of the structure of GAPDH with the cytoplasmic tails bound.

Surface plasmon resonance (SPR) analyses (Fig. 4) confirmed the pulldown assay results. RH1, RH2b, and RH4 showed binding to aldolase, whereas EBA175 and JESEBL were found not to bind (data not shown). The individual association (k_a) and dissociation (k_d) rate constants were obtained by global fitting of data using 1:1 kinetics or the two-state reaction model using BIAevaluation (Biacore, Inc.) (32). Values were then used to calculate the binding affinity according to the equation $K_D = k_a/k_d$ for 1:1 kinetics or the equation $K_D = (k_{a1}/k_{d1}) \times (k_{a2}/k_{d2})$ for the two-state model. The two-state model was found to better fit the data for TRAP, RH1, and RH4, suggesting a change in the conformation during binding. It is a complex binding mechanism involving one binding site with a two-step reaction where an intermediate encounter complex (aldolase: peptide) is observed before the final state is reached. However, this can also arise for other reasons, such as the multimeric nature of aldolase. The K_D values obtained for RH1 and RH4 peptides were found to be lower, i.e., the binding was stronger than that for TRAP (Table 2), although they do not have the tryptophan near the C terminus. This is in contrast to the tryptophan mutant data, which showed that binding was 50 to 100 times weaker when TRAP W was mutated to Y or $F_{(9)}$. These data show clearly that the binding motif in these proteins can be different from the TRAP binding motif but equally effective. RH2B showed very low association and dissociation rates compared to the others; also it had a better fit with 1:1 kinetics. The K_D value obtained was higher, indicative of weaker binding compared to that of the others.

SPR analysis of GAPDH with BAEBL showed a K_D value of 461 nM by two-state kinetics (Fig. 4; Table 2). For RH1, RH4, and JESEBL peptides, GAPDH demonstrated binding, but the curves

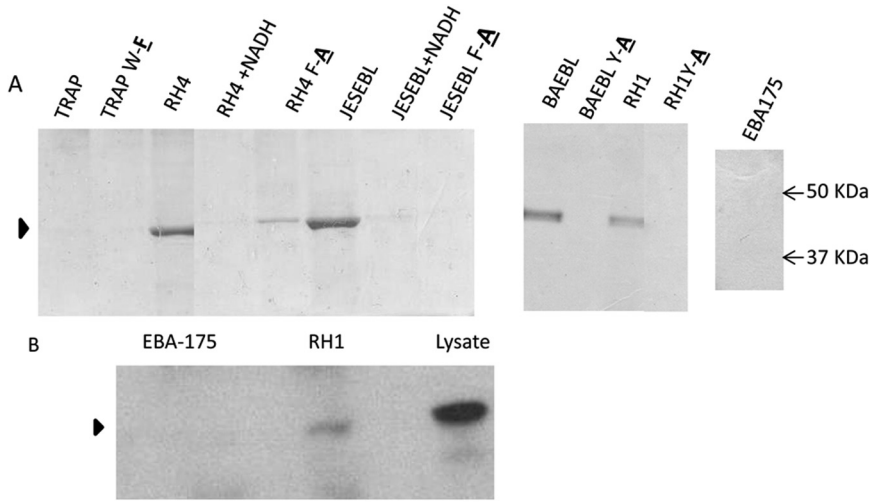

FIG 3 (A) Coomassie-stained gels show the binding of biotinylated peptides containing the C terminus of BAEBL, JESEBL, RH4, RH1, and TRAP to yeast GAPDH in the presence or absence of its cofactor NADH. The mutant residues are bold and underlined. Standards 50 kDa and 37 kDa are marked with arrows. (B) Immunoprecipitation of schizont extracts with rabbit antibodies to EBA175 and RH1 followed by Western blotting with mouse anti-GAPDH antibody. Arrowheads mark GAPDH in panels A and B.

did not fit the 1:1 or the two-state kinetic model. Therefore, we could not determine a K_D for GAPDH binding to those peptides.

P. falciparum aldolase (Pfaldolase) was cocrystallized in the presence of the RH2b peptide (Fig. 5). Analysis of available Pfaldolase structures (1A5C, 2EPH, 2PC4) from the Protein Data Bank with our RH2b cocrystallized aldolase structure indicates an outward movement of α_2 and a downward movement of α_3, whereas α_{13} resides in a rather fixed position (Fig. 5A and B). These structural rearrangements are similar to those observed in TRAP-bound *P. falciparum* structures and distinct from those of unliganded Pfaldolase. Our analysis of the movements of α2 and α3 is suggestive of Pfaldolase interacting with the RH2b peptide despite a lack of interpretable electron density in that region. The positional errors inherent in any high-resolution (HR) X-ray structure for the given resolution range are between 0.05 and 0.15 Å for the Cα position of the residue. Our observed shifts of Cα atoms in α2 were significantly larger than the positional error would allow given a resolution of 2.5 Å and represented excellent electron density for helix 2. For the RH2b cocrystal structure, the average Cα shift for residues K47 to I51 is 1 Å (Fig. 5C). We therefore conclude that the data indicate the presence of a partly occupied binding site. Modeling of the RH2b peptide was omitted due to weak density for the suspected peptide-binding region. Possibly, the crystallization conditions were not optimal for binding of this particular ligand and the results from SPR underlined the weak binding compared to that seen with TRAP. A similar perplexing result was previously described where cocrystallization of *P. falciparum* TRAP failed with *P. falciparum* aldolase but *P. berghei* TRAP with *P. falciparum* aldolase yielded an interpretable electron density map for the *P. berghei* TRAP peptide (8).

In conclusion, our results open the possibility that the binding of aldolase and GAPDH to the cytoplasmic tails of ligands plays a cooperative role in invasion. Such cooperation and different modes of expression of ligands require that many can bind to actin through the bridging molecules. Thus, unlike *P. vivax*, which has only one DBL and a few RH proteins, *P. falciparum* has multiple ligands that can substitute for each other such that mutations in erythrocytes cannot lead to refractoriness to *P. falciparum*.

MATERIALS AND METHODS

Peptide synthesis. The sequences of the C-terminal peptides of the Reticulocyte Homology ligands (RH family) RH1 (PF3D7_0402300), RH2a (PF3D7_1335400), RH2b (PF3D7_1335300), and RH4 (PF3D7_0424200), Duffy Binding-Like (DBL family) ligands, EBA175 (cAMP [GenBank M93397.1] or 3D7 [PF 3D7_0731500]), EBA140, or BAEBL (PF3D7_1301600), and EBA181 or JESEBL (PF3D7_0102500) Thrombospondin-Related Anonymous Protein (TRAP PF13_0201) and their mutants were synthesized with an N-terminal biotin tag. A 6-carbon aminohexanoic acid (Ahx) linker was added after the biotin to the N terminus of the peptide (Biosynthesis or American Peptide). The sequences of the peptides and mutants are shown in Table 1.

Aldolase and GAPDH pulldown assay. Each biotinylated peptide was solubilized in 20 mM Tris-HCl (pH 8.0) (solubilization buffer). To determine the complete solubilization, the solutions were centrifuged at 20,000 $\times$ *g* for 20 min and no pellet was seen. Fifty microliters of peptide solution (0.5 mg/ml) was incubated with 10 μl of streptavidin-agarose beads (Thermo Scientific) in solubilization buffer for 1 h with shaking at room temperature. The beads were washed in solubilization buffer to remove the unbound peptide. Forty micrograms of rabbit muscle aldolase or 40 μg of yeast GAPDH (both from Sigma-Aldrich) was incubated separately with each biotinylated peptide bound to streptavidin agarose beads in 10 mM HEPES (pH 7.5)-50 mM KCl–0.5 mM EDTA–1 mM $MgCl_2$–0.2% Tween 20 (binding buffer) for 4 h at room temperature or overnight at 4°C. For competition assays, the substrate for aldolase, 2 mM fructose-1,6-bisphosphate (Sigma-Aldrich), was added along with 40 μg of aldolase or the cofactor of GAPDH, 10 mM NADH (Sigma-Aldrich), was added to GAPDH. Beads were washed 4 times in binding buffer, and the bound complex was eluted by boiling in reducing SDS loading buffer (NuPAGE lithium dodecyl sulfate [LDS] sample buffer mixed with 10% 2-mercaptoethanol) and analyzed on NuPAGE bis-Tris gels (Invitrogen) (4% to 12%). Precision Plus Protein Dual Xtra standards from Bio-Rad were used as molecular weight markers.

Binding studies using SPR analysis. SPR measurements were made with a BIAcore T100 instrument at 25°C according to the manufacturer's instructions. Sensor CM5, amine coupling reagents, and buffers were pur-

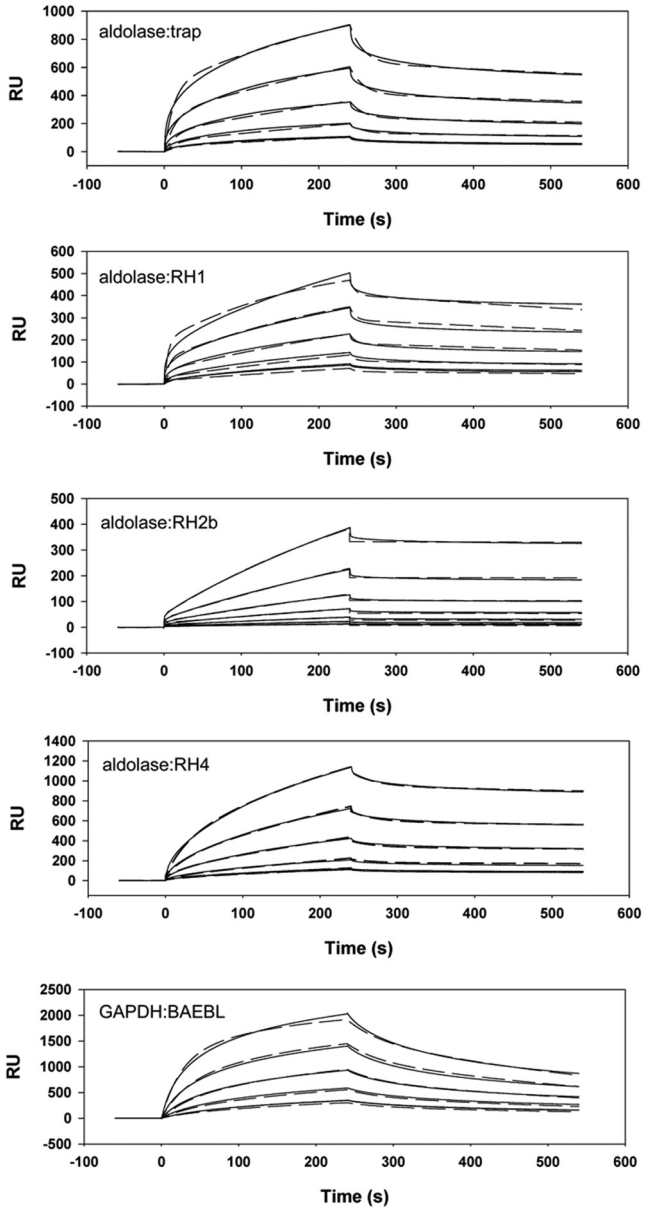

FIG 4 SPR (surface plasmon resonance) sensorgrams of different concentrations of aldolase (50 to 800 nM) and GAPDH (125 to 2,000 nM) binding to C-terminal peptides of different ligands immobilized on a CM5 sensor chip. The experimental data curves and the superimposed results of global-fitting analysis (dotted lines) are shown for RH1, RH2b, RH4, and TRAP. Analysis using 1:1 kinetics was used for RH2B, and two-state kinetics was used for the others. SPR sensorgrams are shown for EBA175 and JESEBL peptides where no binding was seen. RU, resonance units.

chased from GE Healthcare, Piscataway, NJ, unless otherwise noted. The amine cross-linking wizard in T100 control software was used to cross-link all 4 flow cells of the CM5 chip using the following conditions. The CM5 sensor chip was activated with *N*-hydroxysuccinimide (NHS) and 3-(dimethylamino) propyl carbodiimide (EDC) for 7 min. Then, 40 μg/ml NeutrAvidin (Thermo Scientific)-10 mM sodium acetate (pH 5.0) was injected for 7 min followed by blocking with 1 M ethanolamine (pH 8.5) for 7 min. A flow rate of 30 μl/min was used for all steps. The chips were used to immobilize biotinylated peptides. Peptides dissolved in 20 mM Tris (pH 8.0) at a concentration of 0.5 μg/ml were immobilized by passage over an activated CM5 chip at a flow rate of 30 μl/min for 2 min and then washed with a 30-s pulse of 10 mM glycine HCl (pH 2.5). For the binding assay, aldolase or GAPDH was dissolved at different concentrations in 10 mM HEPES (pH 7.5)-0.5 mM EDTA–1 mM $MgCl_2$–0.2% Tween 20 with 100 mM KCl (for aldolase) or 75 mM KCl (for GAPDH). Binding at each concentration was done with an exposure of 4 min followed by 10 min for the dissociation phase. Regeneration was done with a 30-s pulse of 10 mM glycine HCl (pH 2.5). Aldolase substrate F1-6P was added in the buffer to study the effects on binding. All data were collected using a flow rate of 20 μl/min. Blank flow cells with NeutrAvidin immobilized alone (without the biotinylated peptides) were used to subtract the buffer effect on sensorgrams. The kinetic data for aldolase binding were fitted to different kinetic models. BIAcore T100 evaluation software was used for kinetic analysis. The following models were used: the 1:1 Langmuir binding interaction describing 1:1 binding between analyte (A) and ligand (B) ($A + B \leftrightarrow AB$) and a two-state reaction (conformational change) model based on a 1:1 binding of analyte to an immobilized ligand followed by a conformational change ($A + B \leftrightarrow AB \leftrightarrow AB^*$). The individual association (k_a) and dissociation (k_d) rate constants were obtained by global fitting of data using either of the models, whichever fit better.

Production of recombinant RH1 (rRH1) protein and generation of rabbit antisera. The amino acid sequence of recombinant RH1 (rRH1; PlasmoDB accession no. PFL0870w) was used to generate a codon-optimized synthetic gene for expression in *Escherichia coli* (GeneArt, Germany). The construct, corresponding to amino acids 500 to 833 of the full-length gene (previously identified as the minimum binding region of RH1), was subcloned into the *E. coli* pet-24a expression vector downstream of the T7 promoter using the NdeI and XhoI restriction sites (EMD Chemicals). The construct was transformed into *E. coli* BL21(DE3) cells (Novagen, San Diego, CA) and used for rRH1 production. The *E. coli* rRH1 clone was fermented and recovered from inclusion bodies essentially as previously described (33). Inclusion bodies containing rRH1 were solubilized and affinity purified on a nickel Sepharose 6 FF column (GE Healthcare, Piscataway, NJ) following established methods (33). Fractions eluted from the affinity column containing rRH1 were pooled and refolded by rapid dilution at 50 μg/ml protein into a refolding buffer (55 mM Tris [pH 8.2], 264 mM NaCl, 440 mM KCl, 1.1 mM EDTA, 550 mM l-arginine, 440 mM sucrose). The protein was dialyzed overnight in phosphate-buffered saline (PBS) at pH 7.4. Alternatively, for larger-scale refolds, a HiPrep 16/60 Sephacryl S-300 HR refold column (GE Healthcare, Piscataway, NJ) was used that was equilibrated with refolding buffer as the running buffer at a linear flow rate of 30 cm/h, similarly to a previously described method (34). The fractions containing rRH1 were pooled and concentrated by using Amicon Ultra-15 centrifugal filter devices (Millipore, Billerica, MA) (molecular weight cutoff [MWCO], 10 kDa) and polished on a Superdex S75 26/60 SEC column (GE Healthcare) equilibrated with PBS (pH 7.4).

The purity and integrity of rRH1 were determined by Coomassie blue-stained SDS-PAGE under reducing and nonreducing conditions, and the identity of rRH1 was confirmed by N-terminal sequence analysis using Edman degradation (Research Technology Branch; NIH, Rockville, MD). The protein was checked for its erythrocyte-binding activity (data not shown).

Rabbit antisera were generated at the National Institutes of Health in compliance with guidelines of the National Institutes of Health Institutional Animal Care and Use Committee. In brief, rabbits were immunized subcutaneously with 25 μg of rRH1 formulated in Freund's complete adjuvant for priming on day 0 and then incomplete adjuvant for boosting on days 28 and 56. Rabbits were bled on day 84.

Immunoprecipitation assay. *P. falciparum* schizont-infected erythrocytes (5×10^7) were lysed using 0.1% saponin (Sigma-Aldrich)-PBS (pH 7.5)-1 mM phenylmethylsulfonyl fluoride (PMSF; Sigma-Aldrich) for 30 min at 4°C, centrifuged at 20,000 × *g* for 10 min at 4°C, and washed thrice in PBS (pH 7.5)-1 mM PMSF. The released schizonts were resuspended in parasite lysis buffer (1.5 ml of 25 mM HEPES [pH 7.4], 50 mM

TABLE 2 The surface plasmon resonance kinetics for binding of aldolase to the cytoplasmic tails of TRAP, RH1, RH2b, RH4, and GAPDH compared to that of BAEBL[a]

Analyte (bridging molecule)	Ligand (peptide)	k_{a1} ($M^{-1}\ _S\ ^{-1}$)	k_{d1} (s^{-1})	k_{a2} (s^{-1})	k_{d2} (s^{-1})	K_D (nM)
Aldolase	TRAP	3.37E+4	0.052	0.007	5.12E-4	106
	RH1	4.54E+4	0.082	0.018	6.47E-4	61
	RH2b	855.8		1.83E-4		214
	RH4	1.60E+4	0.034	0.012	2.69E-4	47
GAPDH	BAEBL	1.02E+4	0.016	0.008	0.003	461

[a] Kinetic parameters of the rabbit muscle aldolase and GAPDH binding to different peptides were obtained by fitting the concentration-dependent sensorgrams to 1:1 for RH2B or a two-state model for the other peptides. k_a and k_d are association and dissociation rate constants, respectively, and K_D is the binding affinity (in nanomoles) obtained using the following equations: $K_D = k_a/k_d$ (for 1:1 kinetics) and $K_D = (k_{a1}/k_{d1}) \times (k_{a2}/k_{d2})$ (for two-state kinetics). TRAP, Thrombospondin Related Anonymous Protein. RH, reticulocyte homology. $M^{-1}\ s^{-1}$, 1/mole/second.

KCl, 1% Triton X-100, and a protease inhibitor cocktail [Roche Diagnostics]), subjected to a vortex procedure, and kept at 4°C for 4 h with rotating. Every subsequent step was carried out at 4°C. Tubes were centrifuged at 20,000 × *g* for 60 min. Supernatant was collected and preadsorbed for 4 h at 4°C with 200 μl of Dynabeads protein G (Invitrogen) equilibrated in lysis buffer. Aliquots (300 μl) of the supernatant were incubated overnight at 4°C with ~10 to 15 μg of the rabbit anti-Rh1 antibody. Rabbit Rh1-specific antibodies was produced as mentioned above, and anti-EBA175-specific antibodies were kindly provided by Lee Hall and Annie Mo of the Malaria Vaccine Development Section, Division of Microbiology and Infectious Diseases (DMID), NIAID. Dynabeads protein G (40 μl) was added, and the samples were incubated for 4 h at 4°C. Beads were washed four times in 1 ml of lysis buffer and were loaded on NuPAGE bis-Tris gels (Invitrogen) (4% to 12%) after boiling in loading buffer (NuPAGE LDS sample buffer mixed with 10% 2-mercaptoethanol). Gels were transferred overnight onto a 0.2-μm-

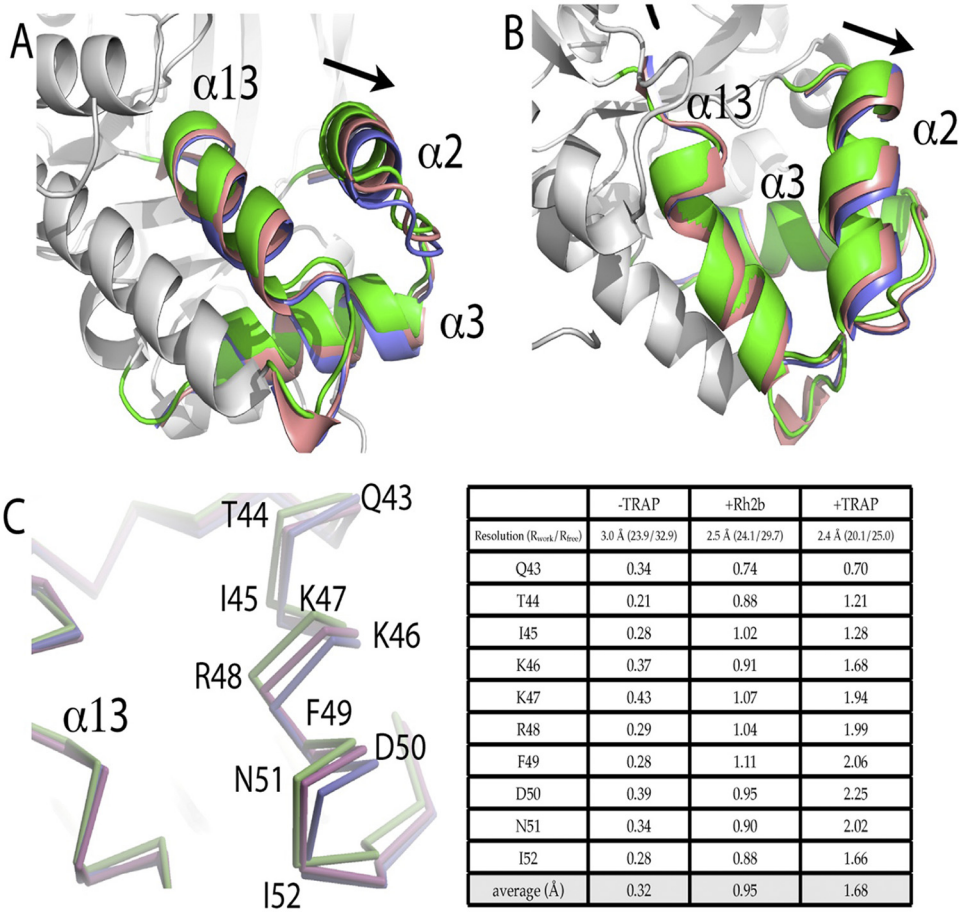

	-TRAP	+Rh2b	+TRAP
Resolution (R_{work}/R_{free})	3.0 Å (23.9/32.9)	2.5 Å (24.1/29.7)	2.4 Å (20.1/25.0)
Q43	0.34	0.74	0.70
T44	0.21	0.88	1.21
I45	0.28	1.02	1.28
K46	0.37	0.91	1.68
K47	0.43	1.07	1.94
R48	0.29	1.04	1.99
F49	0.28	1.11	2.06
D50	0.39	0.95	2.25
N51	0.34	0.90	2.02
I52	0.28	0.88	1.66
average (Å)	0.32	0.95	1.68

FIG 5 (A) Superimposition of 1A5C (uncomplexed *P. falciparum* aldolase) (PfAldolase; green), 2PC4 (TRAP-bound PfAldolase; blue), and RH2b cocrystallized PfAldolase (salmon) shown as a ribbon representation. The overall shift of α2 is indicated with an arrow. (B) View rotated by approximately 90°C along the α2 direction. An outward shift of α2 is visible compared to the uncomplexed structure of 1A5C (green) whereas the α13 helix harboring R309 maintains the same position. (C) Stick representation of the superimposed structures with their relative shifts of Cα position for each residue of α2. Distances are given in angstroms in the table. The first column (TRAP) compares the two chains in 1A5C to each other, representing the expected average noise in the position of α2. The RH2b crystal structure indicates an average movement three times greater than that calculated for the differences between chain A and chain B in 1A5C.

pore-size nitrocellulose membrane (Invitrogen) and probed with mouse *P. falciparum* GAPDH-specific antibodies (gift from Claudia Daubenberger) followed by secondary goat anti-mouse horseradish peroxidase (HRP) (Invitrogen) and developed using SuperSignal West Pico chemiluminescent substrate (Thermo Scientific).

Cocrystallization and data collection of *P. falciparum* aldolase (PfAldolase) in the presence of RH2b. Protein expression, purification, and crystallization of PfAldolase were performed as described in reference 8. RH2b peptide was added in concentrations ranging from 1 mM to 5 mM before setup of crystallization experiments. Crystals grew to approximate dimensions of 80 by 80 by 120 μm and diffracted to 2.5-Å resolution at a synchrotron facility. They belonged to space group $P2_12_12_1$, with unit cell dimensions of a = 71.58, b = 140.53, c = 144.3 α, and β, $\gamma = 90°$.

Structural superimposition of *P. falciparum* aldolase structures. The PDB coordinates 1A5C (35), 2PC4, 2EPH (8), and SSM were superimposed using phenix ensembler (36) and used to get an overall fit following least-squares (LSQ) superposition in Coot using residues 140 to 230 of each of the coordinates. The resulting superposition was visualized using PyMol (http://www.pymol.org). Shifts of Cα positions for residues K46 to I52 were obtained from Coot (37).

ACKNOWLEDGMENTS

We thank Claudia Daubenberger for mouse anti-GAPDH antibody, Annie Mo and Lee Hall (DMID) for rabbit anti-EBA175 antibody, and Susan Pierce for suggestions on the manuscript. Jurgen Bosch thanks Graeme Card, Pete Dunten, Ana Gonzalez, and the staff at SSRL beamlines 9-2 and 12-2 for their help and assistance during synchrotron data collection.

This work was partially funded through the Bloomberg Family Foundation. This study was supported in part by the Intramural Research Program of the National Institutes of Health, National Institute of Allergy and Infectious Diseases.

REFERENCES

1. **Ménard R.** 2001. Gliding motility and cell invasion by Apicomplexa: insights from the plasmodium sporozoite. Cell. Microbiol. **3**:63–73.
2. **Aikawa M, Miller LH, Johnson J, Rabbege J.** 1978. Erythrocyte entry by malarial parasites. A moving junction between erythrocyte and parasite. J. Cell Biol. **77**:72–82.
3. **Miller LH, Aikawa M, Johnson JG, Shiroishi T.** 1979. Interaction between cytochalasin B-treated malarial parasites and erythrocytes. Attachment and junction formation. J. Exp. Med. **149**:172–184.
4. **Srinivasan P, et al.** 2011. Binding of plasmodium merozoite proteins RON2 and AMA1 triggers commitment to invasion. Proc. Natl. Acad. Sci. U. S. A. **108**:13275–13280.
5. **Jewett TJ, Sibley LD.** 2003. Aldolase forms a bridge between cell surface adhesins and the actin cytoskeleton in apicomplexan parasites. Mol. Cell **11**:885–894.
6. **Starnes GL, Coincon M, Sygusch J, Sibley LD.** 2009. Aldolase is essential for energy production and bridging adhesin-actin cytoskeletal interactions during parasite invasion of host cells. Cell Host Microbe **5**:353–364.
7. **Buscaglia CA, Coppens I, Hol WG, Nussenzweig V.** 2003. Sites of interaction between aldolase and thrombospondin-related anonymous protein in plasmodium. Mol. Biol. Cell **14**:4947–4957.
8. **Bosch J, et al.** 2007. Aldolase provides an unusual binding site for thrombospondin-related anonymous protein in the invasion machinery of the malaria parasite. Proc. Natl. Acad. Sci. USA **104**:7015–7020.
9. **Buscaglia CA, Penesetti D, Tao M, Nussenzweig V.** 2006. Characterization of an aldolase-binding site in the Wiskott-Aldrich syndrome protein. J. Biol. Chem. **281**:1324–1331.
10. **Moreira CK, et al.** 2008. The plasmodium TRAP/MIC2 family member, TRAP-like protein (TLP), is involved in tissue traversal by sporozoites. Cell. Microbiol. **10**:1505–1516.
11. **Heiss K, et al.** 2008. Functional characterization of a redundant plasmodium TRAP family invasin, TRAP-like protein, by aldolase binding and a genetic complementation test. Eukaryot. Cell **7**:1062–1070.
12. **Baum J, et al.** 2006. A conserved molecular motor drives cell invasion and gliding motility across malaria life cycle stages and other apicomplexan parasites. J. Biol. Chem. **281**:5197–5208.
13. **Uchime O, et al.** 2012. Analysis of the conformation and function of the *Plasmodium falciparum* merozoite proteins MTRAP and PTRAMP. Eukaryot. Cell **11**:615–625.
14. **Miller LH, Baruch DI, Marsh K, Doumbo OK.** 2002. The pathogenic basis of malaria. Nature **415**:673–679.
15. **Wertheimer SP, Barnwell JW.** 1989. *Plasmodium vivax* interaction with the human Duffy blood group glycoprotein: identification of a parasite receptor-like protein. Exp. Parasitol. **69**:340–350.
16. **Dolan SA, et al.** 1994. Glycophorin B as an EBA-175 independent *Plasmodium falciparum* receptor of human erythrocytes. Mol. Biochem. Parasitol. **64**:55–63.
17. **Lopaticki S, et al.** 2011. Reticulocyte and erythrocyte binding-like proteins function cooperatively in invasion of human erythrocytes by malaria parasites. Infect. Immun. **79**:1107–1117.
18. **Bei AK, et al.** 2007. Variant merozoite protein expression is associated with erythrocyte invasion phenotypes in *Plasmodium falciparum* isolates from Tanzania. Mol. Biochem. Parasitol. **153**:66–71.
19. **Okoyeh JN, Pillai CR, Chitnis CE.** 1999. *Plasmodium falciparum* field isolates commonly use erythrocyte invasion pathways that are independent of sialic acid residues of glycophorin A. Infect. Immun. **67**:5784–5791.
20. **Dolan SA, Miller LH, Wellems TE.** 1990. Evidence for a switching mechanism in the invasion of erythrocytes by *Plasmodium falciparum*. J. Clin. Invest. **86**:618–624.
21. **Gaur D, et al.** 2007. Recombinant *Plasmodium falciparum* reticulocyte homology protein 4 binds to erythrocytes and blocks invasion. Proc. Natl. Acad. Sci. U. S. A. **104**:17789–17794.
22. **Stubbs J, et al.** 2005. Molecular mechanism for switching of *P. falciparum* invasion pathways into human erythrocytes. Science **309**:1384–1387.
23. **Arnold H, Henning R, Pette D.** 1971. Quantitative comparison of the binding of various glycolytic enzymes to F-actin and the interaction of aldolase with G-actin. Eur. J. Biochem. **22**:121–126.
24. **Arnold H, Pette D.** 1968. Binding of glycolytic enzymes to structure proteins of the muscle. Eur. J. Biochem. **6**:163–171.
25. **Daubenberger CA, et al.** 2003. The N′-terminal domain of glyceraldehyde-3-phosphate dehydrogenase of the apicomplexan *Plasmodium falciparum* mediates GTPase Rab2-dependent recruitment to membranes. Biol. Chem. **384**:1227–1237.
26. **Dobrowolski JM, Sibley LD.** 1996. Toxoplasma invasion of mammalian cells is powered by the actin cytoskeleton of the parasite. Cell **84**:933–939.
27. **Field SJ, et al.** 1993. Actin in the merozoite of the malaria parasite, *Plasmodium falciparum*. Cell Motil. Cytoskeleton **25**:43–48.
28. **Pinder JC, et al.** 1998. Actomyosin motor in the merozoite of the malaria parasite, *Plasmodium falciparum*: implications for red cell invasion. J. Cell Sci. **111**(Pt 13):1831–1839.
29. **Gilberger TW, Thompson JK, Reed MB, Good RT, Cowman AF.** 2003. The cytoplasmic domain of the *Plasmodium falciparum* ligand EBA-175 is essential for invasion but not protein trafficking. J. Cell Biol. **162**:317–327.
30. **Singh S, Alam MM, Pal-Bhowmick I, Brzostowski JA, Chitnis CE.** 2010. Distinct external signals trigger sequential release of apical organelles during erythrocyte invasion by malaria parasites. PLoS Pathog. **6**:e1000746.
31. **Dvorin JD, Bei AK, Coleman BI, Duraisingh MT.** 2010. Functional diversification between two related *Plasmodium falciparum* merozoite invasion ligands is determined by changes in the cytoplasmic domain. Mol. Microbiol. **75**:990–1006.
32. **Morton TA, Myszka DG, Chaiken IM.** 1995. Interpreting complex binding kinetics from optical biosensors: a comparison of analysis by linearization, the integrated rate equation, and numerical integration. Anal. Biochem. **227**:176–185.
33. **Shimp RL, Jr, et al.** 2006. Production and characterization of clinical grade *Escherichia coli* derived *Plasmodium falciparum* 42 kDa merozoite surface protein 1 (MSP1(42)) in the absence of an affinity tag. Protein Expr. Purif. **50**:58–67.
34. **Plassmeyer ML, et al.** 2009. Structure of the *Plasmodium falciparum* circumsporozoite protein, a leading malaria vaccine candidate. J. Biol. Chem. **284**:26951–26963.
35. **Kim H, Certa U, Döbeli H, Jakob P, Hol WGJ.** 1998. Crystal structure of fructose-1,6-bisphosphate aldolase from the human malaria parasite *Plasmodium falciparum*. Biochemistry **37**:4388–4396.
36. **Adams PD, et al.** 2011. The Phenix software for automated determination of macromolecular structures. Methods **55**:94–106.
37. **Emsley P, Cowtan K.** 2004. Coot: model-building tools for molecular graphics. Acta Crystallogr. D Biol. Crystallogr. **60**:2126–2132.